JCTC Journal of Chemical Theory and Computation

Article

pubs.acs.org/JCTC

Pushing the Limits of a Molecular Mechanics Force Field To Probe Weak CH···π Interactions in Proteins

Arghya Barman, Bruce Batiste, and Donald Hamelberg*

Department of Chemistry and the Center for Biotechnology and Drug Design, Georgia State University, Atlanta, Georgia 30302-3965, United States

Supporting Information

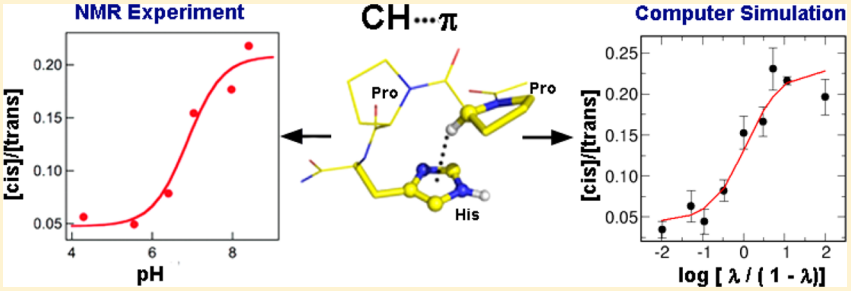

ABSTRACT: The relationship among biomolecular structure, dynamics, and function is far from being understood, and the role of subtle, weak interactions in stabilizing different conformational states is even less well-known. The cumulative effect of these interactions has broad implications for biomolecular stability and recognition and determines the equilibrium distribution of the ensemble of conformations that are critical for function. Here, we accurately capture the stabilizing effects of weak CH···π interaction using an empirical molecular mechanics force field in excellent agreement with experiments. We show that the side chain of flanking C-terminal aromatic residues preferentially stabilize the *cis* isomer of the peptidyl-prolyl bond of the protein backbone through this weak interaction. *Cis*−*trans* isomerization of peptidyl-prolyl protein bond plays a pivotal role in many cellular processes, including signal transduction, substrate recognition, and many diseases. Although the *cis* isomer is relatively less stable than the *trans* isomer, aromatic side chains of neighboring residues can play a significant role in stabilizing the *cis* relative to the *trans* isomer. We carry out extensive regular and accelerated molecular dynamics simulations and establish an approach to simulate the pH profile of the *cis*/*trans* ratio in order to probe the stabilizing role of the CH···π interaction. The results agree very well with NMR experiments, provide detailed atomistic description of this crucial biomolecular interaction, and underscore the importance of weak stabilizing interactions in protein function.

INTRODUCTION

A long-sought goal in the study of biomolecular structure, dynamics, and function is to be able to accurately describe and predict biomolecular interactions using computer simulations. These molecular interactions are critical in stabilizing the folded (native) conformations of proteins, in molecular recognition, and in the description of biological function on the molecular level. Accurately describing biological processes involving biomolecular interactions, which are at times very subtle, using computational simulations requires the need to have an excellent atomic-level representation of the potential energy of the system. The use of empirical molecular mechanics force fields in molecular dynamics simulations has come a long way and can capture very complex regulatory mechanism in biomolecules, including accurately folding entire proteins.[1−4] Nonetheless, limitations of molecular mechanics force fields undoubtedly still exist and have not been rigorously tested in their ability to accurately capture subtle, weak interactions in biomolecules. Assessment of these limitations is usually hampered in many ways by a lack of converged sampling of the conformational phase space of biological systems of interest.

Notoriously slow conformational fluctuations in proteins dynamics, such as *cis*−*trans* isomerization of the peptidyl-prolyl bonds, provide local and global modulation of the conformations of proteins while regulating critical biomolecular processes.[5,6] The *cis* isomer of the peptide bond is rare in protein structures. However, peptidyl-prolyl bonds have higher propensity (∼5%) to adopt the *cis* conformation than nonprolyl peptide bonds (∼0.3%), according to analysis of nonredundant protein structures in the Protein Data Bank.[6−9] *Cis*−*trans* isomerization of peptidyl-prolyl bonds has therefore been shown to act as molecular switches in biomolecular function.[10] The uncatalyzed *cis*−*trans* interconversion is extremely slow and can be the rate-limiting step in the folding and unfolding of proteins.[11] In solution, *cis*−*trans* isomerization proceeds through an energetically high free energy barrier of ∼20 kcal/mol,[12] and the *trans* isomer is ∼ <1 kcal/mol more stable than

Received: November 20, 2014
Published: March 6, 2015

DOI: 10.1021/ct501036r
J. Chem. Theory Comput. 2015, 11, 1854−1863

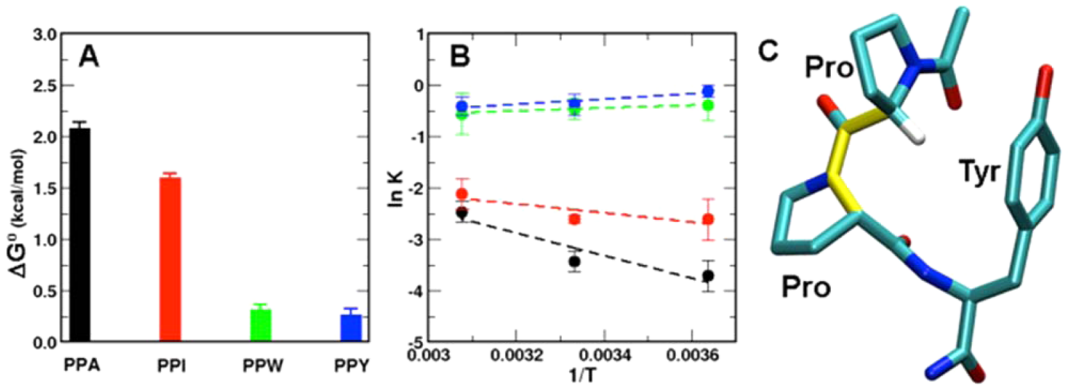

Figure 1. (A) Free energy (ΔG° in kcal/mol) change from the *trans* to the *cis* isomer of a PPX motif (where X is Ala, Ile, Trp, or Tyr). (B) Temperature dependence study and van't Hoff plot of PPA (black), PPI (red), PPW (green), and PPY (blue). (C) Representation of the possible Cα–Hα of the first Pro directed toward the π-ring of the Tyr. The peptidyl-prolyl (ω-) bond is shown in yellow.

the *cis* isomer in a linear peptide. Several families of ubiquitous class of enzymes, known collectively as peptidyl-prolyl *cis*–*trans* isomerases, catalyze and speed the rate of *cis*–*trans* isomerization of the peptidyl-prolyl bond to relevant biological millisecond time scales and regulate numerous biological processes.[13−16] *Cis*–*trans* isomerization therefore plays pivotal roles in signal processing, ion channel opening, substrate recognition, and several other cellular processes[10,17,18] and has been implicated in many diseases if it is not properly regulated.[19]

Although the *trans* isomer, in general, is energetically more favorable than the *cis* isomer, the side chains of flanking residues have been suggested to stabilize the *cis* isomer.[9,20] More specifically, experiments on model peptides and statistical analysis of protein structures in the Protein Data Bank show that proteins containing -Aro-Pro-, -Pro-Pro-Aro-, and -X-Pro-Aro- motifs, where Aro is an amino acid with an aromatic side chain and X is any amino acid, tend to have higher propensity to adopt *cis*-Aro-Pro, *cis*-Pro-Pro, and *cis*-X-Pro peptidyl-prolyl conformations, respectively, suggesting the existence of a favorable interaction between the *cis*-Pro and the Aro side chain.[6,7,9,21,22] In a comparative study many years ago, Grathwohl and Wüthrich showed that the prolyl Phe-Pro bond had higher propensity to be in the *cis* conformation than prolyl nonaromatic-Pro bonds.[23] Similarly, structural analysis of peptides containing Tyr-Pro and Trp-Pro motifs showed *cis* contents that were even greater than that of the Phe-Pro motif.[20,24−28] On the basis of these observations, the more favored *cis* conformation of the peptidyl-prolyl Aro-Pro bond was considered to be due to a weak CH···π interactions between the hydrogen atoms of the Pro residue and the electron-rich π cloud of the aromatic ring.[21,29−34]

Recently, Ganguly et al. have teased out the possible role of the CH···π interaction in stabilizing the *cis* conformation of the -Pro-Pro- peptide bond using detailed NMR experiments on short Ac-Pro-Pro-X-NH_2 peptide motifs.[35] Each peptide can adopt four possible detectable isomeric states (tt, tc, ct, and cc), where t and c correspond to *trans* and *cis*, respectively, due to the inherent isomerization of Ac-Pro and Pro-Pro peptidyl-prolyl bonds. The *cis*/*trans* conformational equilibrium of Ac-Pro is shown to be largely independent of the nature of X. However, the *cis* content of the peptidyl-prolyl bond of Pro-Pro is highly dependent on X. Ganguly et al. show that the free energy difference between the *trans* and *cis* isomers of the Pro-Pro peptide bond is <0.9 kcal/mol when X is Phe, Tyr, Trp, and His (neutral).[35] When X is nonaromatic or His (protonated), the free energy difference between the *trans* and *cis* configurations is ∼2 kcal/mol, resulting in a remarkable decrease in the *cis* content as compared to that when X is aromatic. NMR rotating-frame Overhauser enhancement (ROE) cross-peaks along with the use of molecular models suggest an interaction between Cα–Hα of the N-terminal Pro residue and the ring current of an aromatic side chain when the Pro-Pro peptidyl-prolyl bond is in the *cis* configuration, stabilizing the *cis* conformation through CH···π interaction.[35] This hypothesis is bolstered by a pH-dependent study when X is His. The Pro-Pro peptidyl-prolyl bond of Ac-Pro-Pro-His-NH_2 has a higher *cis* content at higher pH (neutral His) and a lower *cis* content at lower pH (protonated His) with a pK_a of ∼6.8, providing extra stability to the *cis* conformation at higher pH. The pH-dependent *cis* content, when X is His, is due to the fact that protonated His is a poorer π-electron donor in the hypothesized CH···π interaction. These studies provide strong evidence that side chains of flanking residues can have tremendous impact on the conformational dynamics of proteins, biomolecular recognition, and folding and assembly of protein structures as a result of the cumulative effects of subtle and weak interactions.

RESULTS AND DISCUSSION

Considerable progress has been made with NMR experiments in addressing the contributions and stabilizing effects of weak inter- and intramolecular interactions. However, atomic-level understanding of these interactions is not always obvious from current experimental techniques. On the other hand, it is not even clear whether these interactions can be reliably captured using current simulations approaches. Molecular dynamics simulations face two major challenges in accurately capturing these types of interactions. One is the microsecond time scale limitation, and the other is the limitation of the molecular mechanics force field and its ability, or lack thereof, to accurately capture subtle interactions. In order to be able to make meaningful predictions and, for example, fold proteins to their native structures using molecular dynamics simulations, it is important to be able to capture these subtle interactions that, at times, determine the correct distribution of the conformational ensemble. However, in order to adequately address inaccuracies in the force field, the sampling problem has to be resolved, as deviation of simulation results from experiments could simply be due to insufficient sampling. Over the years,

DOI: 10.1021/ct501036r
J. Chem. Theory Comput. 2015, 11, 1854−1863

tremendous efforts have been focused on force field development, and noticeable progress has been made in optimizing force field parameters to reproduce experimental observations.[36−44] Although current force filed parameters show promise in capturing subtle, weak interactions in biomolecules using simulation methods,[45] conformational sampling of long time scale processes beyond microseconds, such as *cis*−*trans* switching of peptidyl-prolyl bond, remains a challenge and still requires the use of advanced simulation methods. Proper assessment of the effectiveness of current force fields, therefore, cannot be achieved without adequate sampling of the conformational space. Here, we push and explore the bounds of a molecular mechanics force field using accelerated molecular dynamics[40,46,47] to investigate the stabilizing role of the weak, subtle CH···π interaction. The results are compared to NMR experiments. In this study, we use a recent nonpolarizable molecular mechanics force field (ff14SB) that comes with the AMBER 14 suite of programs and has evolved through successive modifications of previous AMBER force fields[39,41,42,48,49] combined with the reoptimized parameters for the peptide bond dihedral angle.[40] We also establish a simple, but interesting, approach to determine the equilibrium constants from the pH-dependent *cis*/*trans* equilibrium of the Pro-Pro peptide bond of -Pro-Pro-His- when His is neutral and protonated. All of the simulations were carried out on the peptides used in the NMR experiments, Ac-Pro-Pro-X-NH_2 (PPX), where X is aliphatic (Ala and Ile), aromatic (Trp and Tyr), or histidine (neutral and protonated).

The free energies differences between the *trans* and *cis* isomers of PPA, PPI, PPW, and PPY, shown in Figure 1A, are 2.04 ± 0.11, 1.56 ± 0.08, 0.28 ± 0.08, and 0.23 ± 0.12 kcal/mol, respectively. The simulation results, including the trend between the aromatic and aliphatic residues, and absolute free energies are in excellent agreement with the NMR experimentally measured free energies. The corresponding experimental free energies are 1.52, 1.56, 0.59, and 0.35 kcal/mol, respectively.[35] Error bars for the experiments are not available. Overall, the simulation results clearly show that the *cis* isomer of the peptides with aromatic residues (PPW and PPY) is considerably more stable than that of the peptides with aliphatic residues (PPA and PPI), relative to the *trans* isomer (Figure S1). The results suggest that the aromatic ring is involved in stabilizing the *cis* isomer due to a favorable interaction between the Cα−Hα and the aromatic ring, as shown in Figure 1C. This interaction is lost in PPA and PPI, leading to a less stable *cis* isomer.

Can the force field also capture the temperature dependence of the free energy? Experimentally, the temperature dependence of the free energy change of the aromatic peptides is different from that of the aliphatic peptides. Experimentally and according to the van't Hoff equation, $\ln K = -\Delta H^\circ/RT + \Delta S^\circ/R$, where K is the equilibrium constant, $\Delta G^\circ = -RT \ln K$, R is the gas constant, and T is the temperature, the *cis*/*trans* equilibrium for the aromatic residues (PPW and PPY) is enthalpically driven (ΔH° is negative, and the slope of the plot is positive) and that of the aliphatic residues is not (ΔH° is positive, and the slope of the plot is negative). We carried out simulations using PPA, PPI, PPW, and PPY at three different temperatures starting from 275 to 325 K at 25 K intervals. The van't Hoff plots for the four peptides are shown in Figure 1B. The change in enthalpy (ΔH°; negative of the slope) for PPY and PPW from *trans* to *cis* is calculated to be −1.05 and −0.59 kcal/mol, respectively, suggesting a favorable interaction upon going to the *cis* from the *trans* conformation. The corresponding experimental changes in enthalpy are −1.1 and −1.7 kcal/mol, respectively, in excellent agreement. The calculated changes in entropies (ΔS°) for PPY and PPW are −4.11 and −2.94 cal/mol/K from *trans* to *cis*, also in excellent agreement with experimental values of approximately −4.5 cal/mol/K for both peptides. The calculated changes in enthalpies for PPA and PPI are 4.36 and 1.72 kcal/mol, respectively, and are larger than the experimental estimates. The corresponding experimental enthalpies are ∼0.6 kcal/mol for both peptides. As expected, since the free energies are similar to experiments at 300 K, the calculated entropy changes for PPA and PPI are 8.24 and 0.89 cal/mol/K, respectively, and are also larger than the experimental estimate of approximately −3 cal/mol/K for both peptides. The simulation results reproduce the experimental trend very well. *Trans* to *cis* isomerization of the aromatic peptides is enthalpically driven, whereas that of the aliphatic peptides is not, consistent with the NMR experiments. However, the calculated changes of the enthalpy and entropy for the aromatic peptides are better reproduced than those of the aliphatic peptides. Our results suggest that the proposed CH···π interaction is better captured by the force field than the Lennard-Jones (van der Waals) interactions. The results imply that the effects and free energy changes of the aromatic residues in stabilizing the *cis* configuration can be accurately captured at various temperatures. On the other hand, the free energy change of the aliphatic peptide is accurately captured only at ∼300 K. The Lennard-Jones interaction parameters seem to work best for room-temperature simulations and not other temperatures. Lennard-Jones parameters have actually been suggested to be dependent on temperature.[50] The effect of the Lennard-Jones parameters are not seen in the aromatic peptides because the stronger proposed CH···π interaction, which depends on the distribution of partial charges in a fixed charged molecular mechanics force field, is more dominant in the aromatic side chains and shows the correct temperature dependence.

Furthermore, a pH-dependent simulation study of *cis*−*trans* isomerization of PPH is carried out to test the ability of the force field to accurately capture the CH···π interaction and independently provide an estimate of the equilibrium constants of the *cis*/*trans* equilibrium when His is fully protonated and neutral. The CH···π interaction is expected to depend on the protonation state of His, which is stronger for neutral His and weaker for protonated His. Ganguly et al. showed, using a pH titration study, that the *cis* content of the Pro-Pro peptide bond of Ac-Pro-Pro-His-NH_2 varies with pH.[35] Carrying out molecular dynamics simulations at constant pH is becoming a reality.[51−55] However, it is still a challenge to carry out constant pH simulations in explicit water coupled with enhanced sampling molecular dynamics methods. Progress has been made using implicit solvation.[56] In this study, we have developed an approach by carrying out accelerated molecular dynamics simulations of PPH at various fractions of protonation that is controlled by a variable, λ (0.01, 0.08, 0.16, 0.25, 0.50, 0.75, 0.90, 0.95, and 0.99). Lambda (λ) controls a linear perturbation of the partial charges between neutral and protonated His. Several accelerated MD simulations were carried out at various values of λ between 0 and 1 (0.01, 0.08, 0.16, 0.25, 0.50, 0.75, 0.90, 0.95, and 0.99) but not at λ = 0 and λ = 1. When λ = 0, His is neutral, and when λ = 1, His is protonated. Equations 1 and 2 allow us to then determine the equilibrium constants at λ = 0 and λ = 1,

DOI: 10.1021/ct501036r
J. Chem. Theory Comput. 2015, 11, 1854−1863

instead of directly carrying out simulations at $\lambda = 0$ and $\lambda = 1$, providing a test of the accuracy of the force field parameters, reproduction of the experimental titration curve without assuming the equilibrium constants at $\lambda = 0$ and $\lambda = 1$, and convergence of the simulations by sampling at other values of λ. Equation 1 (see the Supporting Information for derivation) shows the pH dependence on the [*cis*]/[*trans*] ratio.

$$\frac{[cis]}{[trans]} = \frac{K_{tc}^{P} + K_{tc}^{N}\left(\frac{1+K_{tc}^{P}}{1+K_{tc}^{N}}\right)10^{(pH-pK_a)}}{1 + \left(\frac{1+K_{tc}^{P}}{1+K_{tc}^{N}}\right)10^{(pH-pK_a)}} \quad (1)$$

where K_{tc}^{P} and K_{tc}^{N} are the *cis*/*trans* equilibrium constants when His is protonated ($\lambda = 1$) and neutral ($\lambda = 0$), respectively. pK_a is the pK_a of His. According to the Henderson−Hasselbalch equation, $pH - pK_a = \log([\text{neutral}]/[\text{protonated}])$ at a particular λ; therefore, $pH - pK_a$ can be substituted by $\log[\lambda/(1-\lambda)]$ in eq 1 to give eq 2 (see the Supporting Information for derivation).

$$\frac{[cis]}{[trans]} = \frac{K_{tc}^{P} + K_{tc}^{N}\left(\frac{1+K_{tc}^{P}}{1+K_{tc}^{N}}\right)10^{\log\left(\frac{\lambda}{1-\lambda}\right)}}{1 + \left(\frac{1+K_{tc}^{P}}{1+K_{tc}^{N}}\right)10^{\log\left(\frac{\lambda}{1-\lambda}\right)}} \quad (2)$$

The [*cis*]/[*trans*] ratio at different values of λ is calculated using accelerated MD and plotted against $\log[\lambda/(1-\lambda)]$ in Figure 2. The plot clearly shows a dependence of the *cis*/*trans* ratio on the protonation state of His, in excellent agreement with the pH titration curve in the experimental study.[35] The data is fitted to eq 2, and K_{tc}^{P} and K_{tc}^{N} are estimated to be 0.045 and 0.22, respectively, also in excellent agreement with the fit from the NMR experiments of 0.041 and 0.21, respectively. The inflection point is approximately at around $\log[\lambda/(1-\lambda)] = 0$, as expected. On the basis of these simulation results, the additional stability provided by the hypothesized CH···π is $\Delta\Delta G^{\circ} = -RT \ln K_{tc}^{P}/K_{tc}^{N} = 0.95$ kcal/mol at 300 K. The experimental estimate is 0.82 kcal/mol at 277 K.

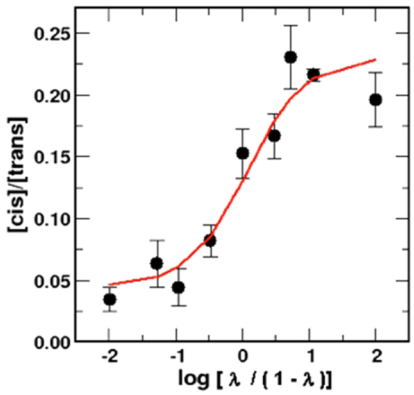

Figure 2. Plot of the *cis*/*trans* ratio of the PPH motif with respect to the $\log[\lambda/(1-\lambda)]$ values. $\lambda = 0$ corresponds to neutral histidine, whereas $\lambda = 1$ signifies the protonated state of histidine. The standard errors are calculated from running the simulations in triplicate.

The energetics of the simulation results are in excellent agreement with experiments, including the remarkable quantitative agreement between the experimental pH profile and the simulated pH profile of PPH. These subtle CH···π interactions at play are surprisingly captured by a non-polarizable molecular mechanics force field. Analysis of the trajectories will therefore provide more conclusive information on the nature of the stabilizing interactions. ROE-NMR cross-peaks between the Cα−Hα of the first proline of PPX, when X is aromatic, and the aromatic ring of X also suggest the existence of the stabilizing CH···π interaction.[35] As estimated above, the CH···π interaction, which is weak and ∼1 kcal/mol, can be considered as a hydrogen bond between the polarized C−H bond and the π-electron clouds of the aromatic ring system.[57] Even though an individual CH···π is weak, collectively, just as a traditional hydrogen bond, CH···π interactions can have significant impact on crystal packing,[58,59] molecular recognition,[60−62] and structure and function of biomolecules.[63,64] Therefore, being able to accurately capture and describe these types of stabilizing interactions are overarching goals in molecular mechanics force field development. We have analyzed our simulation trajectories for the CH···π interaction and investigated the dynamics using PPY. Two-dimensional free energy profiles of the Pro-Pro peptidyl-prolyl bond angle and the distance between the Hα of the first Pro and the center of the ring (RC) of the side chain of Tyr and the Cα−Hα−RC angle are shown in Figure 3. The degrees of freedom monitored during the simulations are shown in Figure 3A. The distance between Hα and RC varies between 2.5 and 12 Å, suggesting that the side chain of Y is flexible and can sample many different conformations. When the Pro-Pro peptidyl-prolyl bond is in the *cis* state, the distance between Hα and RC is ∼3 Å in the dominant conformation of PPY (Figure 3B). A minor population is centered ∼7 Å, with a free energy barrier of ∼2 kcal/mol separating the major and minor conformations. In the *trans* state, the distance between Hα and RC is defined in a broad basin that is centered around 8 Å and between 5 and 11 Å. The results show that the interaction between the Hα of Pro and the side chain of Y is indicative of a CH···π interaction and present in the *cis* conformation but not in the *trans* conformation. If the interaction is mainly CH···π when the peptidyl-prolyl bond is in the *cis* state, then the angle Cα−Hα−RC (θ) should be closer to 180°. Figure 3C shows that, on average, the angle is ∼140°. The angle is also ∼140° when the distance between Hα and RC is ∼3 Å, but it is very broad with a well at ∼50° when the distance is greater than 3 Å (Figure 3D), suggesting that the interactions at a distance of ∼3 Å are CH···π-type interactions in the *cis* conformation.

To further probe the existence of a CH···π interaction between the Hα of the first Pro and the side chain of the aromatic residues, we carried out two simulations on protonated and neutral PPH. As discussed above, the side chain of neutral His is more aromatic than that of protonated His. The overall feature of the free energy profile is similar to that of PPY (Figures 3 and 4). However, noticeable differences are observed between neutral and protonated PPH. Going from neutral PPH (Figure 4A) to protonated PPH (Figure 4B), the free energy basin around 3 Å become less populated and the basin around 7 Å is now almost isoenergetic to the basin around 3 Å. The charge distribution on the ring, and hence the aromaticity, therefore plays a critical role in populating the *cis* conformation around 3 Å, stabilizing a possibly CH···π interaction when His is neutral. The results agree with the pH-dependent *cis* content of the simulation and NMR results. The results also suggest that, irrespective of the protonation states of the His ring, Hα of the first Pro can still come in close proximity to the His ring, also in agreement with the NMR experiments,[35] but the strength of the interaction is weaker when His is protonated.

DOI: 10.1021/ct501036r
J. Chem. Theory Comput. 2015, 11, 1854−1863

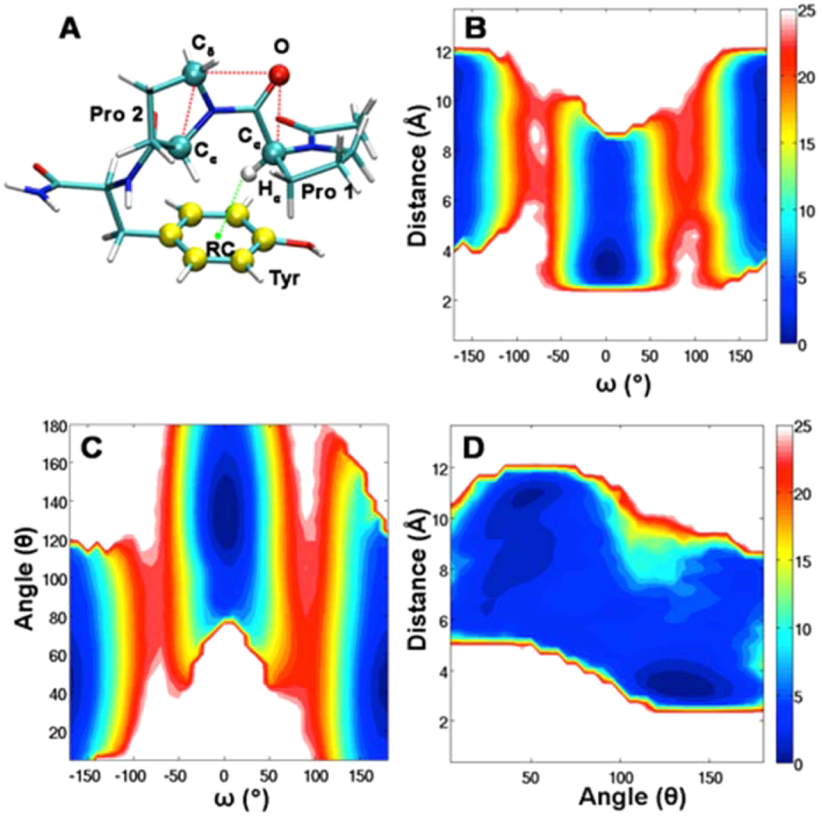

Figure 3. (A) Atomic model of the PPY peptide. The dihedral angle ω (deg) for the *cis*−*trans* isomerization is measured using the dihedral angle between the first Pro (Pro1) and second Pro (Pro2) using Cα, O, Cδ, and Cα atoms (red dots). The distance between the Hα of the first Pro and the ring center (RC) of Tyr is shown with green dots. The Cα and Hα of the first Pro and RC of the Tyr is used to measure the angle θ. (B) Free energy profile of the dihedral angle ω (deg) and the distance. (C) Free energy profile of dihedral angle ω (deg) and the angle (θ). (D) Free energy profile of the angle (θ) and the distance. Free energy is in kcal/mol.

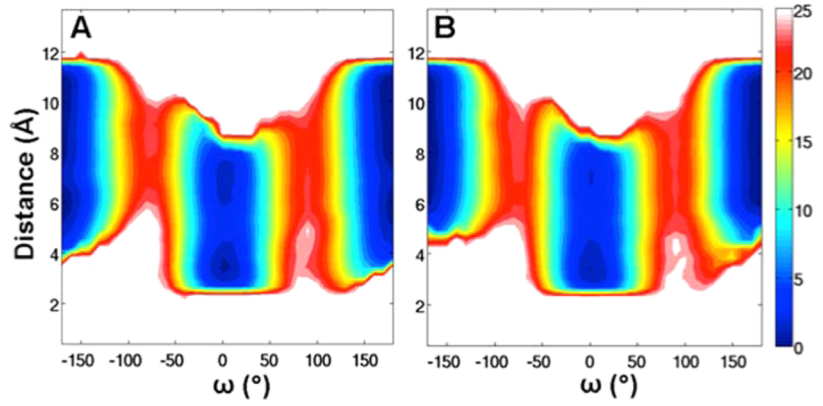

Figure 4. Free energy profile of the dihedral angle ω (deg) and the distance (Hα−RC) in the PPH motif. (A) Histidine in the motif is neutral. (B) Histidine in the motif is protonated. Free energy is in kcal/mol.

Is the CH···π interaction, therefore, the only key *cis*-specific stabilizing interaction in Pro-Pro-Aro motifs? Theoretical investigation of the Pro-Leu-Trp motif in Villin headpiece mini-protein suggests that dispersion interactions can have significant contribution to the total interaction energy between the side chains of Pro and Trp and that only ∼40% of the total interaction energy comes from CH···π interaction.[65] We carried out an additional accelerated molecular dynamics simulation with the PPY peptide, setting the partial charges of all of the atoms to zero to eliminate key electrostatic interactions, in order to shed light on this question. The basin around a Hα−RC distance of ∼3.0 Å is less populated (Figure S2) but continues to be the lower free energy basin when the peptide is in the *cis* conformation, suggesting that dispersion interactions may also contribute to stabilizing the *cis* conformation. We then used only the *cis* conformation of the peptide and ran four regular MD simulations (not accelerated) with varying modification of the key partial charges in order to further probe the importance of dispersion interactions. Regular MD ensures that the conformation stays in the *cis* state, since the barrier separating the *cis* and *trans* states is very high (∼20 kcal/mol). In the first simulation (Figure 5A), all atomic charges

DOI: 10.1021/ct501036r
J. Chem. Theory Comput. 2015, 11, 1854−1863

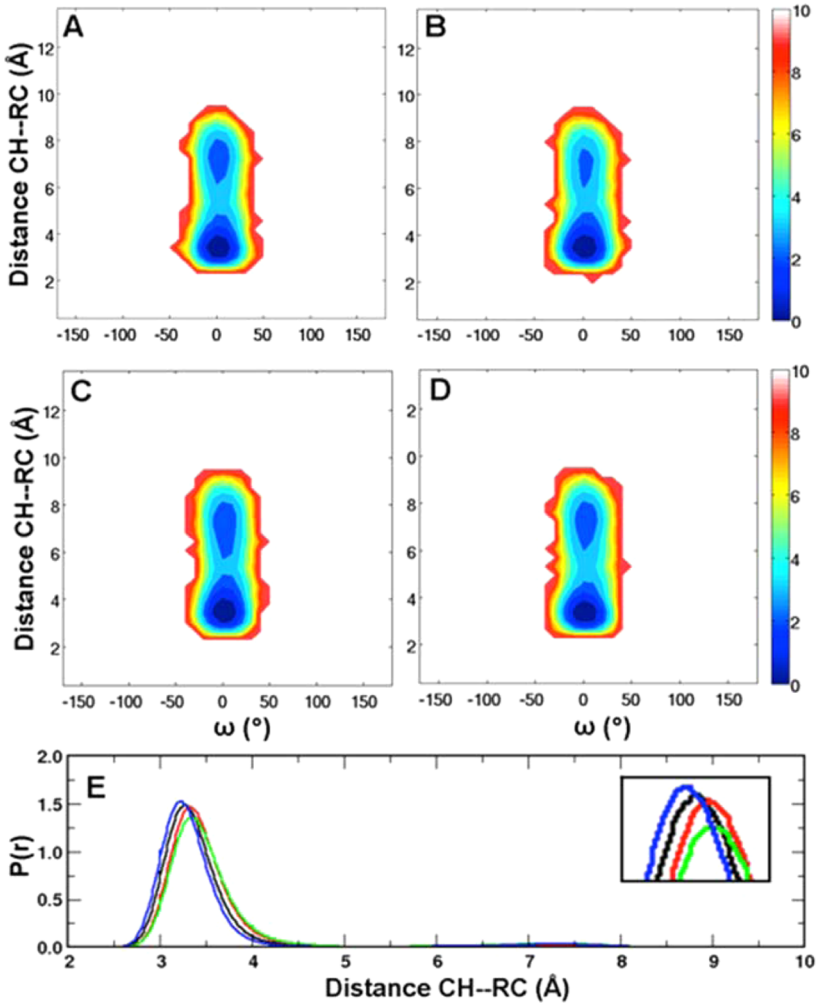

Figure 5. Free energy profile of the distance (Hα−RC) and dihedral angle ω (deg) of PPY in the *cis* conformation from regular MD simulations. (A) Unmodified partial charges. (B) The charge of the Hα of the first Pro is set to zero. (C) Charges of the Hα atom and the hydrogen atoms of the first Pro facing the Tyr ring are set to zeros. (D) Charges of Hα, hydrogen atoms facing the Tyr ring, and the N of the first Pro are set to zeros. (E) Probability distribution of the distance between the Hα of the first Pro1 and RC of Tyr under varying conditions of partial charges: A (black), B (red), C (green), and D (blue). The zoomed-in maximum probabilities are shown in the inset.

were retained. In the second simulation (Figure 5B), only the partial charge on the Hα of the first Pro was set to zero. In the third simulation (Figure 5C), the partial charges on the Hα and all of the hydrogen atoms facing Tyr of the first Pro were set to zero. In the fourth simulation (Figure 5C), all of the partial charges in the third simulation along with the partial charge on the N atom of the first Pro were set to zero. The free energy profiles of all the simulations clearly show similar basins sampled by the *cis* conformation in the accelerated MD simulations. In all the simulations, the conformation with a short distance of ∼3 Å is the most stable, suggesting that in all cases the Hα of the first Pro can come close to the center of the tyrosine ring. However, a plot of the probability distribution of the distance in Figure 5E also shows that there are small, but noticeable, differences among the different simulations.

A small, but consistent, increase in the distance is observed as the weak electrostatic interactions between the proline ring and the ring of Tyr are eliminated by zeroing the partial charges on the Hα and the other hydrogen atoms of the side chain of the first proline. In the fourth simulation, when the partial charge on the nitrogen of the first proline is set to zero, eliminating any possible repulsion with the oxygen of the side chain of Tyr, the distance becomes shorter than that of the first simulation with all of the partial charges. These results therefore suggest that the stabilizing interactions, although primarily dependent on weak CH···π interactions, are also weakly modulated by dispersion interactions. Although CH···π and dispersion interactions could explain the extra stabilization of the *cis* conformation of PPY, the enhanced stability of the *cis* conformation of the GPY motif, lacking any side chain on Gly, raises an interesting question about the role of dispersion interactions in stabilizing the *cis* conformation. In another NMR study, Ganguly et al. showed that after replacing the first Pro with Gly to obtain GPY the *cis* content is similar to that of PPY relative to the *trans* conformation.[66] They concluded that stabilization of the *cis* conformation of GPY, relative to GPA, by ∼0.79 kcal/mol is also entirely due to CH···π interaction between the α-hydrogen atoms of Gly and the aromatic ring of Tyr. GPY therefore can be used to assess whether CH···π is the only interaction responsible for the stabilization of the *cis* conformation. We therefore also carried out two additional regular MD simulations on GPY in the *cis* conformation: one unmodified and the other with the partial charges on the two α-hydrogen atoms set to zero. The time evolution of the distance

DOI: 10.1021/ct501036r
J. Chem. Theory Comput. 2015, 11, 1854−1863

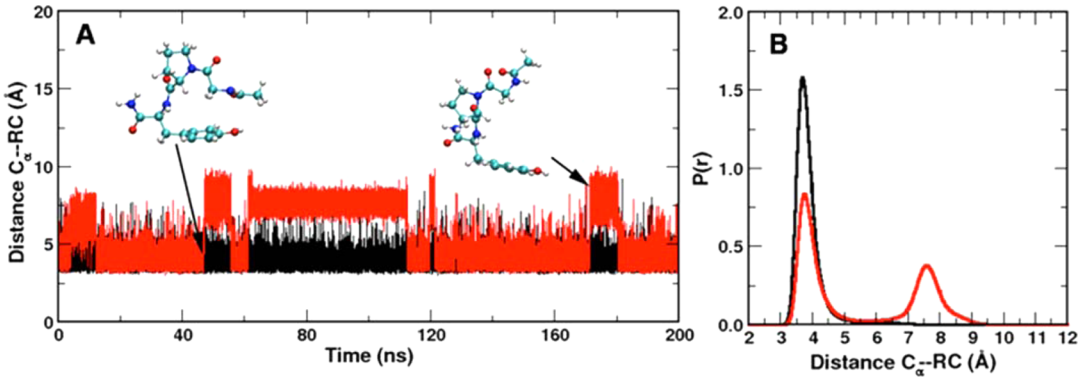

Figure 6. (A) Time evolution and (B) probability distribution of the distance between Cα of the Gly and the RC of the Tyr under varying electrostatic conditions. Unmodified partial charges (black) and when the partial charges of the Hα atoms of Gly are set to zeros.

between the Cα and the center of the aromatic ring (RC) of Tyr is shown in Figure 6A, and the probability distribution is shown in Figure 6B. When the partial charges on the α-hydrogen atoms are unmodified, the distance is short and around 3−4 Å and is consistently formed during the 200 ns of molecular dynamics simulation. When the partial charges on the α-hydrogen atoms are set to zero, the interaction is not consistently formed, suggesting that, indeed, one of the stabilizing interactions is a result of the CH···π interaction. However, the interaction can still form (Figure 6A,B), suggesting that other weak interactions also could marginally contribute to stabilizing the *cis* conformation. These additional interactions are evident in peptides containing the -Aro-Pro-Aro- motif. Interestingly, YPY, FPY, and WPY have higher *cis* content than GPY and PPY according to NMR experiments.[66] In fact, the *cis* conformation of WPY is more stable than the *trans* conformation. In addition to the CH···π interaction, YPY, FPY, and WPY can form an additional stacking interaction between the two aromatic side chains, providing the extra stability that is akin to how the cyclic side chain of proline can interact with the ring of Tyr.

CONCLUDING REMARKS

We have carried out extensive molecular dynamics simulations to assess the ability of an empirical molecular mechanics force field to account for subtle protein interactions. These interactions are the determining energetic interactions in accurately predicting protein−ligand binding and protein−protein recognition and in identifying the dominant conformational states of proteins. Our simulation results confirm the role of CH···π interaction in stabilizing the *cis* conformation of the Pro-Pro-Aro motif and provide an additional atomistic description of the potential role of other subtle hydrophobic (dispersion) interactions. More specifically, our results suggest that CH···π interaction helps to stabilize the *cis* conformation, with dispersion interactions providing additional stabilization. The calculated free energies and the pH-dependent profile of the *cis* content of the Pro-Pro-His motif are in excellent quantitative agreement with experiments. The nonpolarizable molecular mechanics force field parameters (AMBER ff14SB) therefore turn out to be able to quantitatively describe the CH···π interaction that is important for biomolecular structure and function. On the other hand, the results suggest that the Lennard-Jones dispersion parameters (van der Waals interactions) are reliable only at room temperature. More detailed studies may be required to assess the robustness of these weak dispersion parameters at various temperatures. Stabilization of the *cis* conformation by aromatic residues is dominated by the CH···π interaction, which is stronger than the dispersion interactions, and is accurately captured by the fixed partial charges at various temperatures. Interestingly, it has been suggested that Lennard-Jones parameters are dependent on temperature and that an effective potential function might be necessary to remedy this problem.[50] These sorts of detailed simulations and calculations are therefore necessary to assess deficiencies in force fields that can be corrected. However, it is necessary to have converged simulations that can be achieved with advanced simulation methods, such as accelerated molecular dynamics, in order to be sure that lack of sufficient conformational sampling is not being mistaken for deficiencies in the force field parameters.

COMPUTATIONAL METHODS

The peptide models (Ac-Pro-Pro-X-NH_2, where X is Ala, Ile, Trp, Tyr, or His) were constructed using the xleap module in AMBER. The neutral form of His was protonated at the ε nitrogen position, since protonated ε nitrogen is four times more probable and has a slightly higher pK_a (~0.6 pK_a unit) than that of the protonated δ nitrogen.[67] All of the simulations were carried out using the AMBER10[68] suite of programs and performed with the ff14SB force field, which is the latest AMBER force field that comes with the AMBER 14 suite of programs[69] and has evolved through successive modifications of the ff99 and ff99SB force fields,[39,41,42,48,49] combined with the reoptimized parameters for the peptide dihedrals.[40] The systems were solvated in TIP3P[70] water model in an octahedron using the tleap module in AMBER. All bonds involving hydrogen were constrained using the SHAKE algorithm.[71] For the temperature-dependent studies, the systems were equilibrated at their corresponding temperatures (275, 300, and 325 K), and the Langevin thermostat with a collision frequency of 1 ps^{-1} was used to maintain the temperature.[72] The particle mesh Ewald summation method[73] was used to calculate the electrostatic interactions, and a cutoff of 9 Å was used for the nonbonded interactions. All simulations were carried out using the NPT ensemble at a constant pressure of 1 bar, and a time step of 2 fs was used to integrate the equation of motion.

Cis−*trans* isomerization is an extremely slow process, and the time scale is beyond the scope of regular MD simulations. The accelerated molecular dynamcis[40,46] method was used to sample the isomerization process. The rotatable dihedrals

DOI: 10.1021/ct501036r
J. Chem. Theory Comput. 2015, 11, 1854−1863

around the peptidyl-prolyl bond between the first and second prolines were accelerated. The boost potential was set to 20 kcal/mol, and α was set to 0.1 kcal/mol. During the course of accelerated molecular dynamics simulations, a weight of $\exp[\beta\Delta V(r)]$, where β corresponds to $1/k_BT$ (k_B is the Boltzmann constant and T is the temperature), is assigned to each conformation of the peptide. The difference between the modified and unmodified potentials for a particular configuration is $\Delta V(r)$. The probability distribution from the accelerated molecular dynamics simulations was reweighted using $\exp[\beta\Delta V(r)]$. One-dimensional free energy profiles along the peptidyl-prolyl (ω-) dihedral of the peptides were constructed. The free energy profiles were calculated by incrementing each bin size with a value of $\exp[\beta\Delta V(r)]$ if the configuration falls within the bin. The plots were normalized such that the lowest free energy region is 0 kcal/mol. In the 2D profiles, the lowest free energy region (dark blue region) is 0 kcal/mol, and other sampled regions are colored from blue to red. The unsampled regions are colored white. Each simulation was performed for 200 ns in triplicate for proper sampling of the system and calculation of the standard error.

■ ASSOCIATED CONTENT

Supporting Information

Free energy plot of *cis*/*trans* isomerization of the peptides (Figure S1), free energy profile of *cis*/*trans* isomerization of the PPY peptide motif with zero partial charges (Figure S2), and derivation of eqs 1 and 2. This material is available free of charge via the Internet at http://pubs.acs.org.

■ AUTHOR INFORMATION

Corresponding Author

*E-mail: dhamelberg@gsu.edu; Tel.: 404-413-5564; Fax: 404-513-5505.

Funding

This research was support by the National Science Foundation (MCB-0953061). Bruce Batiste was a summer research student from Georgia Perimeter College and was supported by the National Science Foundation (CHE-1262743).

Notes

The authors declare no competing financial interest.

■ ACKNOWLEDGMENTS

This work was also supported by Georgia State's IBM System p7 supercomputer, acquired through a partnership of the Southeastern Universities Research Association and IBM supporting the SURA grid initiative.

■ REFERENCES

(1) Piana, S.; Lindorff-Larsen, K.; Shaw, D. E. Atomic-level description of ubiquitin folding. *Proc. Natl. Acad. Sci. U.S.A.* **2013**, *110*, 5915−5920.

(2) Piana, S.; Klepeis, J. L.; Shaw, D. E. Assessing the accuracy of physical models used in protein-folding simulations: quantitative evidence from long molecular dynamics simulations. *Curr. Opin. Struct. Biol.* **2014**, *24*, 98−105.

(3) Lapidus, L. J.; Acharya, S.; Schwantes, C. R.; Wu, L.; Shukla, D.; King, M.; DeCamp, S. J.; Pande, V. S. Complex pathways in folding of protein G explored by simulation and experiment. *Biophys. J.* **2014**, *107*, 947−955.

(4) Dill, K. A.; MacCallum, J. L. The protein-folding problem, 50 years on. *Science* **2012**, *338*, 1042−1046.

(5) Schulz, G. D.; Schirmer, R. H. *Principles of Protein Structure*; Springer-Verlag: New York, 1979.

(6) Stewart, D. E.; Sarkar, A.; Wampler, J. E. Occurrence and role ofcis peptide bonds in protein structures. *J. Mol. Biol.* **1990**, *214*, 253−260.

(7) MacArthur, M. W.; Thornton, J. M. Influence of proline residues on protein conformation. *J. Mol. Biol.* **1991**, *218*, 397−412.

(8) Wathen, B.; Jia, Z. Local and nonlocal environments around cis peptides. *J. Proteome Res.* **2007**, *7*, 145−153.

(9) Pal, D.; Chakrabarti, P. Cis peptide bonds in proteins: residues involved, their conformations, interactions and locations. *J. Mol. Biol.* **1999**, *294*, 271−288.

(10) Andreotti, A. H. Native state proline isomerization: an intrinsic molecular switch. *Biochemistry* **2003**, *42*, 9515−9524.

(11) Wedemeyer, W. J.; Welker, E.; Scheraga, H. A. Proline cis−trans isomerization and protein folding. *Biochemistry* **2002**, *41*, 14637−14644.

(12) Brandts, J. F.; Halvorson, H. R.; Brennan, M. Consideration of the possibility that the slow step in protein denaturation reactions is due to cis−trans isomerism of proline residues. *Biochemistry* **1975**, *14*, 4953−4963.

(13) Siekierka, J. J.; Hung, S. H. Y.; Poe, M.; Lin, C. S.; Sigal, N. H. A cytosolic binding protein for the immunosuppressant FK506 has peptidyl-prolyl isomerase activity but is distinct from cyclophilin. *Nature* **1989**, *341*, 755−757.

(14) Stamnes, M. A.; Rutherford, S. L.; Zuker, C. S. Cyclophilins: a new family of proteins involved in intracellular folding. *Trends Cell Biol.* **1992**, *2*, 272−276.

(15) Lu, K. P.; Hanes, S. D.; Hunter, T. A human peptidyl-prolyl isomerase essential for regulation of mitosis. *Nature* **1996**, *380*, 544−547.

(16) Fischer, G. Peptidyl-prolyl cis/trans isomerases and their effectors. *Angew. Chem., Int. Ed. Engl.* **1994**, *33*, 1415−1436.

(17) Andreotti, A. H. Opening the pore hinges on proline. *Nat. Chem. Biol.* **2006**, *2*, 13−14.

(18) Sarkar, P.; Reichman, C.; Saleh, T.; Birge, R. B.; Kalodimos, C. G. Proline cis−trans isomerization controls autoinhibition of a signaling protein. *Mol. Cell* **2007**, *25*, 413−426.

(19) Lu, K. P.; Finn, G.; Lee, T. H.; Nicholson, L. K. Prolyl cis−trans isomerization as a molecular timer. *Nat. Chem. Biol.* **2007**, *3*, 619−629.

(20) Reimer, U.; Scherer, G.; Drewello, M.; Kruber, S.; Schutkowski, M.; Fischer, G. Side-chain effects on peptidyl-prolyl cis/trans isomerisation. *J. Mol. Biol.* **1998**, *279*, 449−460.

(21) Bhattacharyya, R.; Chakrabarti, P. Stereospecific interactions of proline residues in protein structures and complexes. *J. Mol. Biol.* **2003**, *331*, 925−940.

(22) Dyson, H. J.; Rance, M.; Houghten, R. A.; Lerner, R. A.; Wright, P. E. Folding of immunogenic peptide fragments of proteins in water solution: I. Sequence requirements for the formation of a reverse turn. *J. Mol. Biol.* **1988**, *201*, 161−200.

(23) Grathwohl, C.; Wüthrich, K. The X-Pro peptide bond as an nmr probe for conformational studies of flexible linear peptides. *Biopolymers* **1976**, *15*, 2025−2041.

(24) Yao, J.; Feher, V. A.; Fabiola Espejo, B.; Reymond, M. T.; Wright, P. E.; Dyson, H. J. Stabilization of a type VI turn in a family of linear peptides in water solution. *J. Mol. Biol.* **1994**, *243*, 736−753.

(25) Kemmink, J.; Creighton, T. E. Local conformations of peptides representing the entire sequence of bovine pancreatic trypsin inhibitor and their roles in folding. *J. Mol. Biol.* **1993**, *234*, 861−878.

(26) Kemmink, J.; Creighton, T. E. The physical properties of local interactions of tyrosine residues in peptides and unfolded proteins. *J. Mol. Biol.* **1995**, *245*, 251−260.

(27) Wu, W.-J.; Raleigh, D. P. Local control of peptide conformation: stabilization of cis proline peptide bonds by aromatic proline interactions. *Biopolymers* **1998**, *45*, 381−394.

(28) Halab, L.; Lubell, W. D. Effect of sequence on peptide geometry in 5-*tert*-butylprolyl type VI β-turn mimics. *J. Am. Chem. Soc.* **2002**, *124*, 2474−2484.

DOI: 10.1021/ct501036r
J. Chem. Theory Comput. 2015, 11, 1854−1863

(29) Satoh, T.; Cowieson, N. P.; Hakamata, W.; Ideo, H.; Fukushima, K.; Kurihara, M.; Kato, R.; Yamashita, K.; Wakatsuki, S. Structural basis for recognition of high mannose type glycoproteins by mammalian transport lectin VIP36. *J. Biol. Chem.* **2007**, *282*, 28246−28255.
(30) Brandl, M.; Weiss, M. S.; Jabs, A.; Sühnel, J.; Hilgenfeld, R. C−H···π interactions in proteins. *J. Mol. Biol.* **2001**, *307*, 357−377.
(31) Nishio, M. CH/π hydrogen bonds in crystals. *CrystEngComm* **2004**, *6*, 130−158.
(32) Umezawa, Y.; Tsuboyama, S.; Takahashi, H.; Uzawa, J.; Motohiro. CH/π interaction in the conformation of peptides. A database study. *Biorg. Med. Chem.* **1999**, *7*, 2021−2026.
(33) Silva, M. M.; Poland, B. W.; Hoffman, C. R.; Fromm, H. J.; Honzatko, R. B. Refined crystal structures of unligated adenylosuccinate synthetase from *Escherichia coli*. *J. Mol. Biol.* **1995**, *254*, 431−446.
(34) Zondlo, N. J. Aromatic−proline interactions: electronically tunable CH/π interactions. *Acc. Chem. Res.* **2012**, *46*, 1039−1049.
(35) Ganguly, H. K.; Majumder, B.; Chattopadhyay, S.; Chakrabarti, P.; Basu, G. Direct evidence for CH···π interaction mediated stabilization of Pro-cisPro bond in peptides with Pro-Pro aromatic motifs. *J. Am. Chem. Soc.* **2012**, *134*, 4661−4669.
(36) Shim, J.; Zhu, X.; Best, R. B.; MacKerell, A. D. Ala_4-X-Ala_4 as a model system for the optimization of the χ1 and χ2 amino acid side-chain dihedral empirical force field parameters. *J. Comput. Chem.* **2013**, *34*, 593−603.
(37) Best, R. B.; Zhu, X.; Shim, J.; Lopes, P. E. M.; Mittal, J.; Feig, M.; MacKerell, A. D. Optimization of the additive CHARMM all-atom protein force field targeting improved sampling of the backbone ϕ, ψ and side-chain χ1 and χ2 dihedral angles. *J. Chem. Theory Comput.* **2012**, *8*, 3257−3273.
(38) Nguyen, H.; Maier, J.; Huang, H.; Perrone, V.; Simmerling, C. Folding simulations for proteins with diverse topologies are accessible in days with a physics-based force field and implicit solvent. *J. Am. Chem. Soc.* **2014**, *136*, 13959−13962.
(39) Hornak, V.; Abel, R.; Okur, A.; Strockbine, B.; Roitberg, A.; Simmerling, C. Comparison of multiple Amber force fields and development of improved protein backbone parameters. *Proteins: Struct., Funct., Bioinf.* **2006**, *65*, 712−725.
(40) Doshi, U.; Hamelberg, D. Improved statistical sampling and accuracy with accelerated molecular dynamics on rotatable torsions. *J. Chem. Theory Comput.* **2012**, *8*, 4004−4012.
(41) Lindorff-Larsen, K.; Maragakis, P.; Piana, S.; Eastwood, M. P.; Dror, R. O.; Shaw, D. E. Systematic validation of protein force fields against experimental data. *PLoS One* **2012**, *7*, e32131.
(42) Wickstrom, L.; Okur, A.; Simmerling, C. Evaluating the performance of the ff99SB force field based on NMR scalar coupling data. *Biophys. J.* **2009**, *97*, 853−856.
(43) Steinbrecher, T.; Latzer, J.; Case, D. A. Revised AMBER parameters for bioorganic phosphates. *J. Chem. Theory Comput.* **2012**, *8*, 4405−4412.
(44) Joung, I. S.; Cheatham, T. E. Molecular dynamics simulations of the dynamic and energetic properties of alkali and halide ions using water-model-specific ion parameters. *J. Phys. Chem. B* **2009**, *113*, 13279−13290.
(45) Gallivan, J. P.; Dougherty, D. A. A computational study of cation−π interactions vs salt bridges in aqueous media: implications for protein engineering. *J. Am. Chem. Soc.* **2000**, *122*, 870−874.
(46) Hamelberg, D.; Mongan, J.; McCammon, J. A. Accelerated molecular dynamics: a promising and efficient simulation method for biomolecules. *J. Chem. Phys.* **2004**, *120*, 11919−11929.
(47) Doshi, U.; Hamelberg, D. Achieving rigorous accelerated conformational sampling in explicit solvent. *J. Phys. Chem. Lett.* **2014**, *5*, 1217−1224.
(48) Graf, J.; Nguyen, P. H.; Stock, G.; Schwalbe, H. Structure and dynamics of the homologous series of alanine peptides: a joint molecular dynamics/NMR study. *J. Am. Chem. Soc.* **2007**, *129*, 1179−1189.
(49) Lindorff-Larsen, K.; Piana, S.; Palmo, K.; Maragakis, P.; Klepeis, J. L.; Dror, R. O.; Shaw, D. E. Improved side-chain torsion potentials for the Amber ff99SB protein force field. *Proteins: Struct., Funct., Bioinf.* **2010**, *78*, 1950−1958.
(50) Nasehzadeh, A.; Mohseni, M.; Azizi, K. The effect of temperature on the Lennard-Jones (6−12) pair potential function. *J. Mol. Struct: THEOCHEM* **2002**, *589*−*590*, 329−335.
(51) Mongan, J.; Case, D. A.; McCammon, J. A. Constant pH molecular dynamics in generalized Born implicit solvent. *J. Comput. Chem.* **2004**, *25*, 2038−2048.
(52) Lee, M. S.; Salsbury, F. R.; Brooks, C. L. Constant-pH molecular dynamics using continuous titration coordinates. *Proteins: Struct., Funct., Bioinf.* **2004**, *56*, 738−752.
(53) Chen, W.; Wallace, J. A.; Yue, Z.; Shen, J. K. Introducing titratable water to all-atom molecular dynamics at constant pH. *Biophys. J.* **2013**, *105*, L15−L17.
(54) Goh, G. B.; Hulbert, B. S.; Zhou, H.; Brooks, C. L. Constant pH molecular dynamics of proteins in explicit solvent with proton tautomerism. *Proteins: Struct. Funct. Bioinform.* **2014**, *82*, 1319−1331.
(55) Goh, G. B.; Knight, J. L.; Brooks, C. L. Constant pH molecular dynamics simulations of nucleic acids in explicit solvent. *J. Chem. Theory Comput.* **2011**, *8*, 36−46.
(56) Williams, S. L.; de Oliveira, C. A. F.; McCammon, J. A. Coupling constant pH molecular dynamics with accelerated molecular dynamics. *J. Chem. Theory Comput.* **2010**, *6*, 560−568.
(57) Tsuzuki, S. CH/π interactions. *Annu. Rep. Prog. Chem., Sect. C: Phys. Chem.* **2012**, *108*, 69−95.
(58) Umezawa, Y.; Tsuboyama, S.; Takahashi, H.; Uzawa, J.; Nishio, M. CHπ interaction in the conformation of organic compounds. A database study. *Tetrahedron* **1999**, *55*, 10047−10056.
(59) Matsumoto, A.; Tanaka, T.; Tsubouchi, T.; Tashiro, K.; Saragai, S.; Nakamoto, S. Crystal engineering for topochemical polymerization of muconic esters using halogen−halogen and CH/π interactions as weak intermolecular interactions. *J. Am. Chem. Soc.* **2002**, *124*, 8891−8902.
(60) Tóth, G.; Kövér, K. E.; Murphy, R. F.; Lovas, S. Aromatic−backbone interactions in α-helices. *J. Phys. Chem. B* **2004**, *108*, 9287−9296.
(61) Kobayashi, K.; Asakawa, Y.; Kato, Y.; Aoyama, Y. Complexation of hydrophobic sugars and nucleosides in water with tetrasulfonate derivatives of resorcinol cyclic tetramer having a polyhydroxy aromatic cavity: importance of guest-host CH−π interaction. *J. Am. Chem. Soc.* **1992**, *114*, 10307−10313.
(62) Frontera, A.; Garau, C.; Quiñonero, D.; Ballester, P.; Costa, A.; Deyà, P. M. Weak C−H/π interaction participates in the diastereoselectivity of a host−guest complex in the presence of six strong hydrogen bonds. *Org. Lett.* **2003**, *5*, 1135−1138.
(63) Spiwok, V.; Lipovová, P.; Skálová, T.; Buchtelová, E.; Hašek, J.; Králová, B. Role of CH/π interactions in substrate binding by *Escherichia coli* β-galactosidase. *Carbohydr. Res.* **2004**, *339*, 2275−2280.
(64) Tatko, C. D.; Waters, M. L. Comparison of C−H···π and hydrophobic interactions in a β-hairpin peptide: impact on stability and specificity. *J. Am. Chem. Soc.* **2004**, *126*, 2028−2034.
(65) Kang, Y. K.; Byun, B. J. Strength of CH···π interactions in the C-terminal subdomain of villin headpiece. *Biopolymers* **2012**, *97*, 778−788.
(66) Ganguly, H. K.; Kaur, H.; Basu, G. Local control of cis-peptidyl−prolyl bonds mediated by CH···π interactions: the Xaa-Pro-Tyr motif. *Biochemistry* **2013**, *52*, 6348−6357.
(67) Reynolds, W. F.; Peat, I. R.; Freedman, M. H.; Lyerla, J. R. Determination of the tautomeric form of the imidazole ring of L-histidine in basic solution by carbon-13 magnetic resonance spectroscopy. *J. Am. Chem. Soc.* **1973**, *95*, 328−331.
(68) Case, D. A.; Cheatham, T. E.; Darden, T.; Gohlke, H.; Luo, R.; Merz, K. M.; Onufriev, A.; Simmerling, C.; Wang, B.; Woods, R. J. The Amber biomolecular simulation programs. *J. Comput. Chem.* **2005**, *26*, 1668−1688.
(69) Case, D. A.; Babin, V.; Berryman, J. T.; Betz, R. M.; Cai, Q.; Cerutti, D. S.; Cheatham, T. E, III; Darden, T. A.; Duke, R. E.; Gohlke, H.; Goetz, A. W.; Gusarov, S.; Homeyer, N.; Janowski, P.; Kaus, J.; Kolossváry, I.; Kovalenko, A.; Lee, T. S.; LeGrand, S.; Luchko, T.; Luo,

DOI: 10.1021/ct501036r
J. Chem. Theory Comput. 2015, 11, 1854−1863

R.; Madej, B.; Merz, K. M.; Paesani, F.; Roe, D. R.; Roitberg, A.; Sagui, C.; Salomon-Ferrer, R.; Seabra, G.; Simmerling, C. L.; Smith, W.; Swails, J.; Walker, R. C.; Wang, J.; Wolf, R. M.; Wu, X.; Kollman, P. A. *AMBER 14*; University of California: San Francisco, CA, 2014.

(70) Jorgensen, W. L. Revised TIPS for simulations of liquid water and aqueous solutions. *J. Chem. Phys.* **1982**, *77*, 4156−4163.

(71) Ryckaert, J.-P.; Ciccotti, G.; Berendsen, H. J. C. Numerical integration of the cartesian equations of motion of a system with constraints: molecular dynamics of *n*-alkanes. *J. Comput. Chem.* **1977**, *23*, 327−341.

(72) Izaguirre, J. A.; Catarello, D. P.; Wozniak, J. M.; Skeel, R. D. Langevin stabilization of molecular dynamics. *J. Chem. Phys.* **2001**, *114*, 2090−2098.

(73) Essmann, U.; Perera, L.; Berkowitz, M. L.; Darden, T.; Lee, H.; Pedersen, L. G. A smooth particle mesh Ewald method. *J. Chem. Phys.* **1995**, *103*, 8577−8593.

DOI: 10.1021/ct501036r
J. Chem. Theory Comput. 2015, 11, 1854−1863